Proteins in Vacuo. Denaturing of Disulfide-Intact and Disulfide-Broken Lysozyme Probed by Molecular Dynamics Simulations

C. T. Reimann,[†] I. Velázquez,[‡] and O. Tapia*[,‡]

Division of Ion Physics, Department of Radiation Sciences, Uppsala University, P. O. Box 535, S-751 21 Uppsala, Sweden, and Department of Physical Chemistry, Uppsala University, P. O. Box 532, S-751 21 Uppsala, Sweden

Received: September 15, 1997; In Final Form: December 30, 1997

Proteins in vacuo are the subject of a number of experimental techniques where unfolding has been shown to be an important feature. In this paper we report on a detailed structural study of protein denaturation modeled in molecular dynamics (MD) simulations of disulfide-intact (DI) and disulfide-reduced (DR) lysozyme (LYZ) molecules at 293 K in vacuo with the GROMOS force field. The trajectories were carried out over at least 1.0 ns in the absence of water molecules, starting from an X-ray structure. A repulsive centrifugal potential was generated for both DI- and DR-LYZ, inducing large conformational transitions. Denaturation followed a pathway eliciting the existence of two well-defined subdomains involving the alpha helixes (designated here as α_1 and α_2) while the beta sheet appeared to comprise a full domain (β). The domain unfolding differed markedly for DI- and DR-LYZ. The unusual structures found in this type of simulation for DI-LYZ were compared with related unfolding simulations in water and were found to be similar to those obtained using radial unfolding forces. Furthermore, the transient structures were compatible with a three state model used to describe unfolding. The present simulation of DI-LYZ would be partly compatible with the results of an experiment on nonequilibrium refolding of DI-LYZ (Miranker, A.; et al. *Science* **1993**, *262*, 896) if the unfolded structures were to belong to a putative refolding pathway. Modeling of structures of protein ions, stored and manipulated in vacuo, is initiated using the information herein presented. The most extended conformer of DI-LYZ derived computationally resembles qualitatively the extended conformers observed experimentally by energetic surface imprinting.

Introduction

Recently, practical questions about the conformation of proteins in vacuo have been raised in the area of biological mass spectrometry,[1−7] where massive biomolecular ions are produced in the gas phase and are made to interact collisionally with surfaces[8] and with nonreactive[9−11] and reactive gases.[12−18] Increasingly often, these mass spectrometry techniques are employed to address specific noncovalent protein−protein,[19] protein−ligand,[20] and protein−nucleic-acid[21] complexes of fundamental importance in biological function and molecular recognition events.

Results of a number of new physical experiments (viz. collision cross section measurements) carried out on biomolecular ions suggest that the conformation of proteins in vacuo can be deliberately varied over a wide range.[22] The analysis of these experiments also yields information about the sizes and shapes of the probed biomolecules. Moreover, protein folding is observed to occur in vacuo,[18,22] although it is not known whether the resulting compact species are closely related to the native conformation. Since it is commonly regarded that protein folding pathways are determined by the amino acid sequence and the environmental conditions, with water playing a strong role,[23,24] the new observations motivate a reassessment of the precise role of water in determining the behavior of proteins. Studies in vacuo would be valuable in elucidating the potential of the sequence itself to determine protein folding, structure, stability, and possibly function.[25]

Considerable physical experimentation in vacuo has focused on a particular protein, hen egg-white lysozyme (LYZ), which is stabilized by four intrachain disulfide bonds. For example, energetic surface imprint studies show that disulfide-intact LYZ (DI-LYZ) and disulfide-reduced LYZ (DR-LYZ) are partly elongated or "sticklike" in the gas phase;[26] measurements of gas-phase basicities and collision cross sections also suggest the existence of a wide range of conformers of DI- and DR-LYZ.[22,27,28] Although these physical methods generally yield the gross conformation of proteins in vacuo, the structural details at the domain, subdomain, and atomic levels remain elusive. Computational methods such as molecular dynamics (MD), seeded with plausible starting structures, can be used to provide detailed information that may shed light on the observed conformational changes.

Motivated in part by a desire to achieve a better detailed understanding of the unusual protein conformations which could be observed in vacuo, we carried out a computational study with the D4 parameter set of the GROMOS force field[29] on DI- and DR-LYZ, both initially present in the native conformation deduced by X-ray crystallography, in the absence of explicitly represented solvent molecules. The difference between this and previous works[30,31] is that we are particularly interested in the vacuum environment (using the D4 parameter set is equivalent to simulating a neutral protein in vacuo, i.e.,

* Corresponding Author. Phone, +46 18-471-3659, FAX, +46 18-508-542; e-mail, Orlando.Tapia@fki.uu.se.
[†] Division of Ion Physics.
[‡] Department of Physical Chemistry.

S1089-5647(97)03011-3 CCC: $15.00
Published on Web 02/26/1998

an NP model[32]), whereas past works have considered the solution phase. The NP model is used successfully to reproduce atomic fluctuations in a neighborhood of the X-ray structure.[32] To achieve this end, two elements of the model are important. The first element is a global electroneutrality, and the second one is a *weak* coupling to a Berendsen thermal bath.[33] For a system that is *strongly* coupled to a thermal bath, it was early found that conformational changes can be induced in modeled proteins.[34] This feature was exploited in the present work to computationally denature both DI-LYZ and DR-LYZ.

The application of GROMOS to proteins in vacuo may be puzzling as this force field is gauged against molecules in solution. It is worth mentioning that in a comparative study, CHARMM was used[35] to simulate an electrically neutral protein in vacuo yielding results similar to GROMOS. One may thus expect that the water-free force field, whose form is independent of the state of aggregation, is a plausible potential to test the response of a protein to disruptive fields in the absence of water or any other solvent. Such disruptive fields are actually produced experimentally by charging the proteins. As a first step, we here use centrifugal forces as the source of disruption. The present simulations may be considered as a first step in the search for a representation of proteins in vacuo. The simulation results are discussed in light of experimental data.

Methods

The atomic coordinates from the crystal structure of wild-type hen egg-white DI-LYZ at 0.17 nm resolution[36] were obtained from the Brookhaven Protein Data Bank (E.C. 3.2.1.17; PDB entry 1hel). The coordinates of the polar hydrogens were generated from standard geometries, leading to a total of 1275 atoms in this simulation.

To simulate DR-LYZ, the same initial coordinates were used as those for DI-LYZ but the appropriate cysteine pairs were unbound from each other and capped with hydrogens. A total of 1283 atoms were used in this simulation (LYZ contains four disulfide bridges).

All computations were carried out using the GROMOS-87 D4 force field.[29] Normally, performing calculations within the NP framework models the electrical shielding of protein charges by H_2O solvent and counterions without including the mass of the solvent. That is the rationale, but it was not intended as an apodictic procedure.[32] For our purposes, the use of NP means that we effectively model the behavior of an electrically neutral protein in vacuo. The *net* charge on any amino acid charge group is zero, although dipoles and multipoles still exist, ensuring the existence of intramolecular electrostatic interactions.

Starting with the coordinates obtained as described above, energy minimizations were carried out with molecular mechanics using the method of steepest descent. Bond-length constraints were provided by SHAKE.[37] For DI-LYZ, the total energy decreased by ≈7000 kJ/mol (73 eV) after 350 iterations. For DR-LYZ, the total energy decreased by ≈17000 kJ/mol (180 eV) after 390 iterations. In both cases, the final total energy was negative.

MD simulations were performed on the structures described above under conditions of constant volume and temperature and with initial atom velocities taken from a Maxwellian distribution characteristic of a temperature of 293 K. A strong coupling to the Berendsen bath was used ($\tau = 0.01$ ps). The time step was 2 fs. Nonbonded interactions were evaluated at every time step for all neighbors within 0.8 nm. Long-range Coulombic interactions between charge groups were cut off at 1.3 nm. The nonbonded pair list was updated, and long-range Coulomb interactions were recalculated every 10 time steps. Periodic boundary conditions were *not* applied. During these simulations the total kinetic energy was constant at about 3000 kJ/mol (30 eV) to within less than 6%. Likewise, the total energy was always less than −8000 kJ/mol (−80 eV). The simulation output trajectories were analyzed to extract energies, root-mean-square (rms) position deviations, principle moments of inertia, radii of gyration, etc.

For the sake of analysis, two domains are defined here as α (residues 1−39 and 88−129) and β (residues 40−87). These definitions are flexible but are essentially equivalent to ones given in the literature.[31,38−40] The α domain may exist in the form of two subdomains, α_1 (residues 1−39) and α_2 (residues 88−129), which have been synthesized as separate peptides and independently studied.[40]

We also describe trends in the behavior of the secondary structure of DI-LYZ and DR-LYZ. To identify the secondary structural features of lysozyme, we employed the helixes listed in the Brookhaven Protein Data Bank for DI-LYZ.[36] The helixes are here labeled H1 (residues 4−16), H2 (25−34), H3 (79−84), H4 (88−100), H5 (104−108), H6 (109−114), and H7 (120−124). The elements of the β-sheet, BS, were determined by inspection of the hydrogen bonding patterns of DI-LYZ and involve residues 42−60. The existence of a hydrogen bond was checked by using a distance criterion between the donor−acceptor centers, taking as a maximum a typical or representative distance of 0.315 nm.[41] A longer distance of 0.415 nm was also used for checking the existence of potential or transient hydrogen bonds.

The analysis of the secondary structural aspects of DI-LYZ and DR-LYZ under the action of centrifugal forces was focused mainly on helixes H1, H2, and H4, the three longest helixes in LYZ, and on the β-sheet BS. The integrity of helixes was analyzed in two ways: by plotting principle moments of inertia (PMIs, calculated using the C_α carbons) and by plotting the number of intrabackbone hydrogen bonds between residue pairs separated by four residues, for each helix. The integrity of the β-sheet BS was analyzed simply by plotting the number of original BS-stabilizing hydrogen bonds surviving as a function of time.

Results

Control Simulation: Weak Coupling to the Berendsen Bath. For DI- and DR-LYZ, a 1-ns MD simulation was performed in the standard fashion. In each case, for the first 10 ps, the whole system was strongly coupled to a Berendsen thermal bath at 293 K with a relaxation time constant of 0.01 ps. Then, the relaxation time was increased to 0.1 ps, weakening the coupling to the thermal bath. For DI-LYZ, rms deviations of the C_α atoms of the MD-simulated structure from those of the X-ray crystallographic structure were at all times less than 0.18 nm, indicating that DI-LYZ is as stable in the NP computational framework as it is in computations carried out explicitly including the solvent.[30] The DR-LYZ trajectory was similarly stable.

Strong Coupling to the Berendsen Bath. Conformational changes in vacuo (i.e., unfolding) in DI-LYZ and DR-LYZ were induced by centrifugal forces that radially perturbed the molecular structure. This effect was achieved with a strong coupling to the thermal bath. In the following, we first describe the general trends in the behavior of the domain (tertiary) structure of DI-LYZ and DR-LYZ during the roughly 1-ns time period of the strongly coupled MD simulations. Thereafter, we

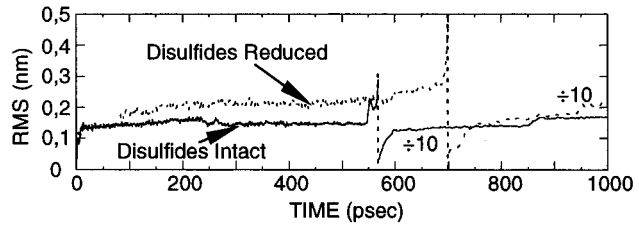

Figure 1. rms deviations of the polypeptide backbone alpha carbons (C_α) of disulfide-intact (DI) and disulfide-reduced (DR) hen egg-white lysozyme (LYZ), resulting from molecular dynamics simulations starting from structures close to the X-ray crystallographic structure of DI-LYZ. The rms values are extracted with respect to the X-ray crystallographic structure of DI-LYZ.

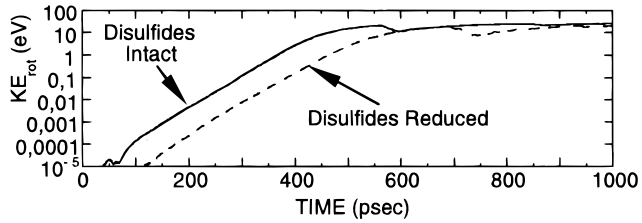

Figure 2. Rotational kinetic energy plotted as a function of time for molecular dynamics simulations of DI- and DR-LYZ. The model proteins are strongly coupled to a Berendsen thermal bath during the whole simulation.

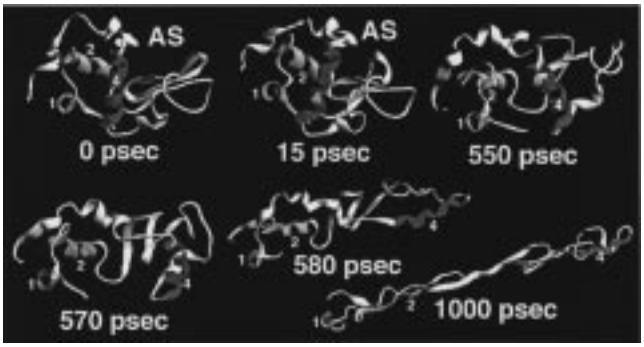

Figure 3. Views of the structure of DI-LYZ at the indicated times. "1" denotes helix H1, "2" denotes helix H2, and "4" denotes helix H4. "AS" denotes active site. The pictures are made with the program Ribbons (M. Carson, University of Alabama at Birmingham, CMC).

present an analysis of the secondary structure elements. Many of these elements dissolved after 600 ps for DI-LYZ while for DR-LYZ their persistence times were somewhat longer.

Disulfide-Intact Lysozyme: Tertiary Structure. Within 15 ps, a loop consisting of residues 43−51 had deflected toward the active site of the protein, covering it. Thereafter, the rms deviations of the C_α atoms of the MD-simulated structure from those of the X-ray crystallographic structure were about 0.15 nm up to a time of around 540 ps (Figure 1). However, the rotational kinetic energy over this time period increased from essentially zero to about 1900 kJ/mol (20 eV) (Figure 2). At 560 ps, the rms deviation suddenly rose to 1.3 nm, indicating that the conformation of the protein had become more open. After a gradual further increase, a second sudden increase in the rms deviation to 1.7 nm occurred at 850 ps.

The general opening of the conformation of DI-LYZ acted on by centrifugal forces is schematically portrayed in Figure 3. H1 is always shown oriented perpendicular to the plane of the figure.

Over the time period 550 to 570 ps, an unhinging type motion was observed, resulting in H1 and H2 moving away from H4. The axis of this unhinging was approximately in the plane of

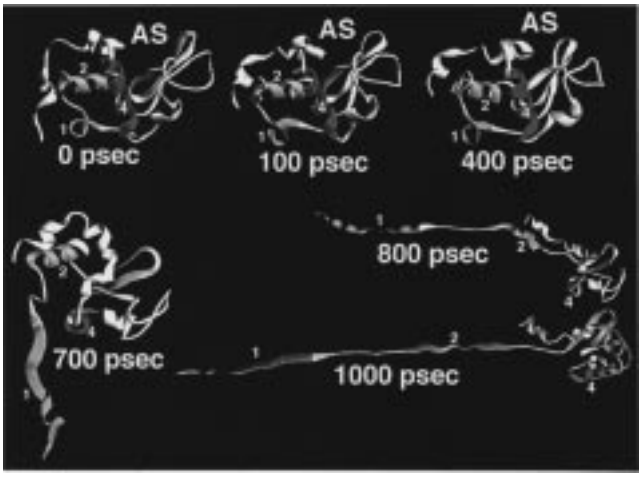

Figure 4. Views of the structure of DR-LYZ at the indicated times. The presentation scheme is the same as in Figure 3.

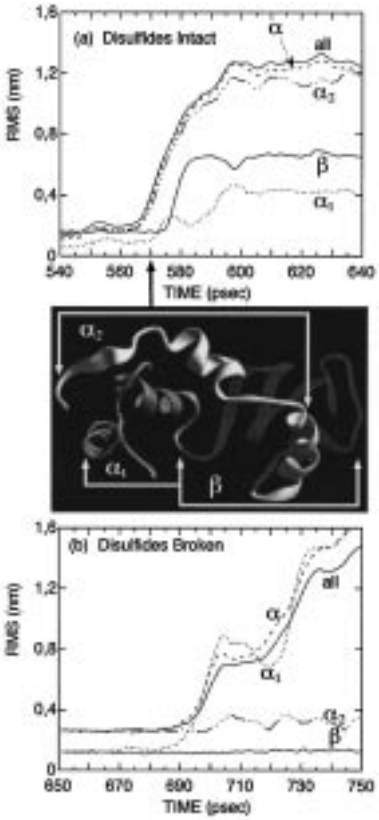

Figure 5. rms deviations of the simulated protein and certain domains and subdomains, calculated with respect to the X-ray crystallographic structure, at the indicated times, for (a) DI-LYZ and (b) DR-LYZ. The α and β domains, and the α_1 and α_2, subdomains, are defined in the text. The middle frame shows a view of the protein structure at time 570 ps for DI-LYZ.

Figure 3 and, as the molecule expanded, it was oriented centrally and perpendicular to the long direction of the molecule. At 580 ps, the protein started to stretch against the disulfide bridges. Since these are not symmetrically placed in the molecule, stresses occurred in the structure. H4 then turned by about 90° to be parallel to the long axis of the molecule. Stretching continued, to the extent that H2 and H4 both ended up being elongated and oriented parallel to the long axis. H1 remained located at one end of the molecule in unstretched form.

The rms deviations for the domains are reported in Figure 5a. The domain α_1 contains both H1 and H2, while α_2 contains

H4. The separation of H4 from H1 and H2 at around 540 ps (Figure 3) thus reflected the denaturation of domain α. There are differences, however, in the behavior of its subdomains. α_2 was strongly denatured while α_1 was only weakly deformed as elicited also by the helix H1 that was preserved over the simulated time. β was also denatured but less severely than the whole protein, α, or α_1. The rms calculations indicate that β and α_1 denatured about 10 ps after α_2, showing that an unhinging motion occurred as α_1 swung away from β, resulting in the stretching of α_2 (Figure 5, middle). It should be noted that this unhinging is different from the hinging motion described by McCammon et al.[42] since we are concerned with a denaturation process and not with the process by which the active site can open and close near the native conformation.[39]

Disulfide-Reduced Lysozyme: Tertiary Structure. Around 90 ps, a subtle but fast increase occurred in the rms value of the whole protein, due to a slight alteration of the protein conformation into a more globular shape. In contrast to the behavior of DI-LYZ, residues 43−51 approached the opposite side of the active site only very slowly, after about 400 ps. The rms deviations were less than 0.22 nm, though slowly increasing, up to a time of around 600 ps (Figure 1), indicating similarity to the X-ray crystallographic structure under that time period. Again, the rotational kinetic energy over this time period increased from essentially zero to about 1900 kJ/mol (20 eV) (Figure 2). Between 690 and 750 ps the rms jumped to 1.4 nm and then slowly increased thereafter, indicating that unfolding had set in. At 940 ps a further sudden jump in rms occurred to 2.1 nm.

The general opening of the conformation of DR-LYZ acted on by centrifugal forces is shown schematically in Figure 4. The behavior is quite different from that of DI-LYZ. In particular, the opening process was delayed until about 690 ps. The polypeptide chain then started to become unraveled from the protein at the N-terminus, the length of the free end increasing over time. H1 and H2 sequentially unraveled from the protein body and then became stretched. At least up to a time of 1.2 ns (the maximum time of this simulation), the final structure was not further deformed.

From Figure 4, it may be surmised that only the subdomain α_1 was denatured, as H1 and H2 but not H4 became unwound from the protein. From Figure 5b, the rms deviations indeed confirm that, around 700 ps, β and α_2 remained similar to the X-ray crystallographic structure (though α_2 displayed notable fluctuations) while α_1 was strongly denatured.

Disulfide-Intact Lysozyme: Secondary Structure. PMIs and hydrogen bonding patterns are plotted for DI-LYZ in Figure 6. By looking at PMI values for all the helixes (only those for H1, H2, and H4 are shown here), major conformational changes were seen to occur at four times: 40, 580, 650, and 850 ps.

At 40 ps, H7 became significantly elongated and displayed considerable variations in conformation at all times thereafter.

At 580 ps, significant conformational changes occurred in H3, H4, and H5, with accompanying transient disturbances in H2 and H7. Changes in H3 and H5 were sudden, while the change in H4 occurred over about 50 ps. Indeed, by 600 ps, no hydrogen-bonding pattern characteristic of the α-helix remained in H4. However, H4 was not completely stretched out: inspection of the structure indicates the partial formation of a 3^{10} helix which persisted over the total remaining time of the MD simulation. The number of hydrogen bonds characterizing the β-sheet BS was preserved at about 60% during the first 550 ps, but by 600 ps the number of these bonds dropped to about 10%, indicating substantial denaturation of BS at that

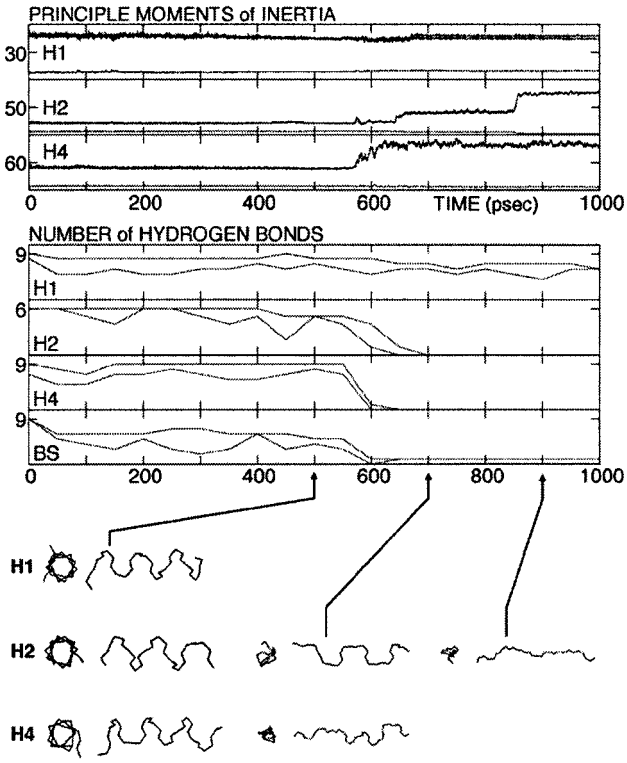

Figure 6. Principal moments of inertia (PMI) and number of surviving hydrogen bonds plotted versus time for the molecular dynamics simulation of DI-LYZ. (For the number of surviving hydrogen bonds, the upper trace uses a relatively large donor−acceptor distance to monitor transient bonds, while the lower trace uses a more typical distance to monitor more stable hydrogen bonds.) Shown at the bottom are end and side views of three of the helixes at one or more times as indicated by the arrows. For these views, the length scales change over time to allow a compact presentation, but by comparing the approximate length-to-width ratios, the degree of stretching of each helix can be ascertained. The helixes are identified and other details discussed in the text.

time. Yet the domain β containing BS maintained some degree of correspondence to the X-ray crystallographic structure (Figure 5a).

At 650 ps, H2 became elongated, correlated with a slight extension of H1. Between 650 and 700 ps, there was a disappearance of the hydrogen bonding pattern characteristic of the α-helix in H2. Inspection of H2 shows that a flat, 3^{10}-like helix persisted between about 650 and 850 ps.

At 850 ps, a further elongation occurred in H2 and in H6. These helixes became completely stretched.

Helix H1 was quite stable for all time, except for a slight elongation mentioned above. About 70% of the hydrogen bonding pattern corresponding to the α-helix conformation was preserved for all time. Correspondingly, the (sub)domain in which H1 resides, α_1, was the most stable with respect to denaturation (Figure 5a).

To summarize, the overall secondary structure was well-preserved until about 550 ps, when major changes also took place in terms of unfolding of the tertiary structure. The changes in the active site region, mentioned above, could not be correlated with any change of secondary structure, and hence the openness of the cleft of the active site was mostly influenced by the interaction between the two major domains α and β. But the gross denaturation induced centrifugally corresponds to α_1 hinging away from β, resulting in the stretching of α_2.

Disulfide-Reduced Lysozyme: Secondary Structure. PMIs and hydrogen-bonding patterns are plotted for DR-LYZ in

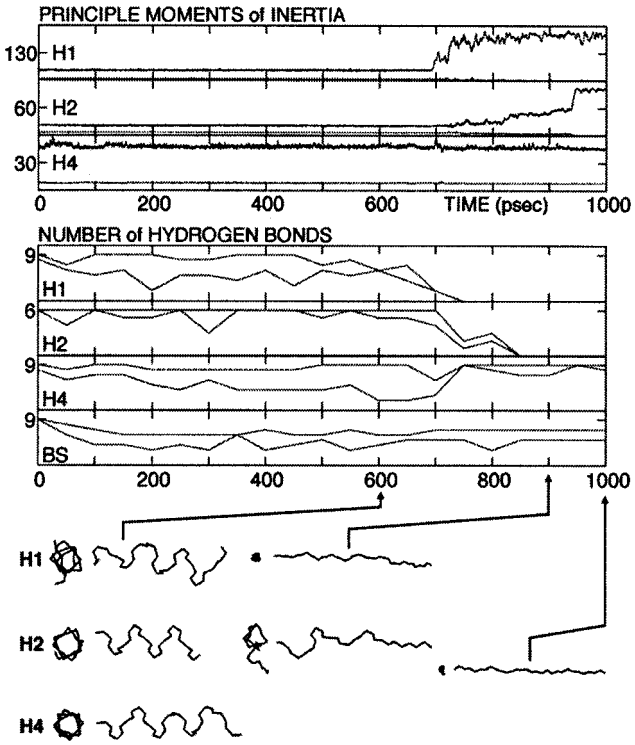

Figure 7. PMIs and number of surviving hydrogen bonds plotted versus time for the molecular dynamics simulation of DR-LYZ. The presentation is the same as in Figure 6.

Figure 7. Over the first 700 ps, PMIs of *all* helixes were rather stable. (There was a small change over the first 15 ps, and, particularly in H6, a larger but still quite small change occurred at about 80 ps. These features are not shown here.)

Between 700 and 750 ps, the PMIs for H1 (Figure 7) indicated an elongation to a stable, fully stretched conformation (Figure 4). Between 700 and 750 ps, the hydrogen-bonding pattern characteristic of an α-helix for H1 was destroyed and never returned during the rest of the simulation.

The PMIs for H2 (Figure 7) show that the stretching of H2 was delayed with respect to that of H1, being initiated at about 720 ps, thereafter continuing slowly until a completely stretched conformation was reached at about 950 ps. The hydrogen-bonding pattern characteristic of an α-helix for H2 was destroyed by time 850 ps and never returned during the rest of the simulation.

All other helixes displayed long-term stability to times of 1 ns and longer. For example, see the PMIs for H4 (Figure 7). However, the PMIs of H4, H5, H6, and H7 (shown only for H4) displayed transient features at times ranging from 700 to 720 ps, when significant conformational changes started occurring in H1 and H2. However, PMIs restabilized in all cases well before the conformations of H1 and H2 reached their final configuration. H3 displayed the most stable PMIs and hydrogen-bonding pattern.

The number of hydrogen bonds characterizing the β-sheet BS was preserved at about 70% for the entire time of the simulation, indicating that this structural moiety was quite stable.

To summarize, all helixes and the β-sheet in DR-LYZ were stable except for H1 and H2, which sequentially unwound from the body of the protein (Figure 4) and became stretched by centrifugal forces. This is in line with the observation of small rms deviations of α_2 and β for all time, as well as large rms deviations of α_1 (Figure 5b).

Discussion

Denaturing simulations using centrifugal forces in vacuo have revealed differential behavior as a function of the disulfide bond state of reduction and also a well differentiated behavior of subdomains. It is of interest to compare the present results with the results of experiments and simulations carried out in both the solution and in vacuo phases.

Comparison with Simulations of Disulfide-Intact Lysozyme in Solution. Computer-simulated denaturation has been carried out with DI-LYZ in the solution phase by Mark and van Gunsteren[30,31] by heating to 500 K. They observe unfolding in a two-stage process. In the first one, secondary structure becomes fleeting: the number of hydrogen bonds involved in forming the α-helixes and the β-sheet begins to fluctuate. In the second stage, there is a loss of α-helicity and β-sheet character, although the hydrogen bonds forming these structures return on a transient basis. Notably, at the end of their simulation (200 ps), the protein is still quite compact, and vestiges of the two domains α and β which form the active site of LYZ are still visible, though these have each expanded and have also moved away somewhat from each other. Even at that stage, a small fraction remains of α-helix-arrayed polypeptide chain. In this kind of denaturation procedure, the "T-run",[31] H1 and H2 shrink, reform, and finally vanish, and H4 shrinks and vanishes. In the centrifugal denaturation technique presented here, by contrast, H1 was preserved, while H2 abruptly vanished and H4 was stretched to form in part a 3^{10} helix (Figure 6). Also, the final conformation reached with centrifugal denaturation was much more stick-like than the final conformation reached in the T-run.

The approach of Hünenberger et al.[31] in attempting to denature DI-LYZ by sharply increasing the pressure (the "P-run") failed in the simulated time to induce denaturation. Thus the centrifugal denaturation method presented here is more effective than a P-run at inducing significant unfolding of DI-LYZ.

Two other approaches for computer denaturation were taken by Hünenberger et al.,[31] constant radial force ("F-run") and kinetic energy gradient ("K-run"). In the F-run, the distance between the centers of mass of the α and β domains increases, as we effectively observed (Figure 3; Figure 5, middle). Also in the F-run, the radius of gyration of α increases significantly, whereas that of β does not, and that is in line with our observation that the most stable domain is β. In the K-run, the protein is observed to split into two sections: β combines with H4 as one section, and the remainder of α appears as the other section. Thus, in the K-run, β remains intact, while α_1 and α_2 separate (α_2 with H4 remaining with β), quite similar to what we observed (Figure 3; Figure 5, middle). In both F- and K-runs, H1 was preserved, while H2 and H4 became relatively elongated. Our centrifugal denaturation method appeared to stretch H2 and H4 more severely than did the F- and K-runs. Indeed, centrifugal denaturation overall produced much more elongated proteins than did either the F- or the K-run. Hünenberger et al.[31] point out that the unfolding events induced by the F-run and the K-run "... suffer from similar biases as will any unfolding scheme depending on the center of mass of the protein".[31] Centrifugal denaturation is indeed an unfolding scheme which depends on the center of mass of the protein. However, because of local stabilization by a disulfide bridge, we observed that H1 was well preserved, even though it is on an outlying portion of the denatured protein.

A notable parallel between our centrifugal denaturation runs and the T-run[31] is that, computationally, relative extremes of

energy are required to affect denaturation. We required rotational energies of the order of 20 eV to centrifugally denature the model protein, far in excess of the energy the global rotational mode would possess in thermal equilibrium at room temperature; and the T-run requires a temperature of 500 K, which would burn a real system. In both cases, it is justifiable to use such an extreme computational tool for speeding up the denaturation process, so it can be achieved in the ns time scale. However, this parallel between two independent MD simulations, both involving the GROMOS-type potentials, may also elicit a too "stiff" potential.

Comparison with Experiments on Disulfide-Intact Lysozyme In Solution. Classically, DI-LYZ is thought to consist of two folding domains, α and β.[31,38−40] However, under centrifugal denaturation in vacuo, α clearly separates into two elements which appear as subdomains, α_1 and α_2 (Figure 3, Figure 5a). Thus, considering the various stages of denaturation, we observed by MD that DI-LYZ occupies *three* unique states (Figure 3) which might be involved in putative refolding: (a) an essentially native form, (b) a form in which α is partly intact (α_1) and partly denatured (α_2) while β is intact, and (c) a form in which all the domains are quite denatured. These results can be compared qualitatively to the results of an experiment by Miranker et al.[43] involving nonequilibrium *refolding* of DI-LYZ in solution, in which mass spectrometry was used to identify *three* unique states of the protein. It was further found[43,44] that, in solution, the α domain folds faster than the β domain, results deduced from measurements of amide hydrogen protection against deuterium exchange. Our results are partly compatible with this picture. For example, in Figure 5a, if the unfolding pathway were to be reversed, α_1 would begin to fold first, followed by β, and then α_2. So, amide protection would occur first in α, though the protection would not be complete in α until after β folded. There are obviously many caveats in comparing protein unfolding and refolding in solution and in vacuo. Protein unfolding and refolding are not necessarily analogous, and also, the time scales of the experiments[43] (milliseconds) and our MD simulations (nanoseconds) are radically different. Still, in the absence of solvent and with a possibly unusual unfolding force, elements of α appear to unfold later than β, partly analogous to the reverse of nonequilibrium refolding observed in solution.[43,44]

Comparison with Experiments on Isolated Subdomains of Lysozyme in Solution. Another line of comparisons appears natural when one looks at the well-differentiated behavior of the subdomains for DR-LYZ perturbed centrifugally in vacuo. There are experimental studies designed to probe the secondary structure of isolated portions of the α domain in the *solution phase*[40] (the isolation of the peptide fragments representing qualitatively the absence of disulfide bridges in DR-LYZ). Experimentally, a peptide containing LYZ residues 1−40 (essentially similar to α_1) was found to possess little secondary structure, mirroring the MD result for DR-LYZ that the secondary structure of α_1 was quickly destroyed. However, a peptide containing LYZ residues 84−129 (quite similar to α_2) was found experimentally to display some secondary structure, although the H4 helix was disordered. This qualitatively mirrors the MD result for DR-LYZ showing high stability of α_2 under centrifugal perturbation (in the experiment, however, α_2 is not accompanied by β and thus may be somewhat destabilized).

Comparison with Experiments on Disulfide-Intact Lysozyme in Vacuo. Recent experiments have addressed the conformation of DI-LYZ ions in the gas phase.[22,26] Radial centrifugal forces are similar to radial forces engendered by Coulomb repulsion for charged protein ions, and therefore the centrifugal denaturation runs presented here can constitute a plausible model for the unfolding of highly charged protein ions in vacuo. Reimann et al.[26] derived an overall length of 13.5 nm for DI-LYZ in the charge state $Q = 9+$, qualitatively similar to the length 11 nm of the centrifugally denatured DI-LYZ after 1 ns of strongly coupled MD. This extended conformer may be similar to one observed by Valentine et al.[22] to be characterized by a collision cross section about 67% greater than that of the native structure; those authors used energetic injection of DI-LYZ in charge states around $Q = 9+$ into a bath gas to drive an unfolding process. If the computer-generated structure were found to belong to a class of structures observed experimentally, the ability of GROMOS-type potentials to accurately model the behavior of proteins in vacuo would be validated to a certain degree. Preliminary work for DI-LYZ strongly suggests that such might be the case, though existing experimental data for DI-LYZ in vacuo only admit a comparison at the tertiary structural level.

Comparison with Experiments on Disulfide-Reduced Lysozyme in Vacuo. Computational denaturation of DR-LYZ led to considerably extended albeit lopsided conformers (Figure 4). Comparing with gas-phase conformers studied experimentally for DR-LYZ,[22,26] however, no correlation with our MD results was found, since the simulated conformers were considerably shorter (16 nm) than those observed in energetic surface imprinting experiments (26−32 nm).[26] For DR-LYZ, unfolding in vacuo may occur via a different route than that driven by centrifugal forces. Furthermore, the initial state affected by Coulomb repulsion may not be one closely similar to the native state, as assumed in our centrifugal denaturation simulations reported here.

Why Do Denaturation Modes for DI-LYZ and DR-LYZ Differ? Computational denaturation of DR-LYZ has not been previously attempted. We found that a much greater fraction of the secondary and even tertiary structure of DR-LYZ was preserved compared to DI-LYZ, a surprising result considering that all the intrachain disulfide bridges are absent in DR-LYZ and that complete elongation of the polypeptide chain might have been expected. As pointed out above, strong coupling to a thermal bath yields a nonstationary trajectory for the internal degrees of freedom of the protein, even though the total kinetic energy is constant. Thus, there is a flow of energy from the internal degrees of freedom to *collective* rotational and vibrational motion. This flow of energy is strongly modulated by the ease with which energy flows among the internal degrees of freedom, which in turn is strongly dependent on how "spring-like" motifs (i.e., α-helixes and β-sheet) are fastened together.[45] Breaking the fastening points (viz. disulfide bridges) makes the protein structure more loose and "floppy", and may result in better localization of vibrational energy and less efficient transfer of energy to the global rotational and vibrational modes. Centrifugal denaturation is hence delayed for DR-LYZ and the specific manifestation of denaturation in terms of the final structure is completely altered. A rigorous study of the collective rotational and vibrational motion of proteins is beyond the scope of the present paper but would form an interesting topic for future research. One prediction upon which such research would have bearing is that changes in certain excitation states of proteins, called "wringons", can cause changes in the state of the protein itself[46] (i.e., in its conformation).

Conclusions

We have applied here a complementary means of computationally denaturing a protein in vacuo: centrifugal denaturation

via a strong coupling of the protein to an external perturbing source modeled as a thermal bath. The method is sensitive to the presence or absence of disulfide bridges, which strongly affected the form of denaturation undergone by otherwise structurally equivalent proteins. Much more secondary and tertiary structure was maintained if the disulfide bridges were absent.

For disulfide-intact lysozyme, results of in vacuo molecular dynamics simulations suggested the existence of three unique conformational states, qualitatively resembling three *solution-phase* states identified by mass spectrometry.[43] And for disulfide-reduced lysozyme, the simulations suggested that the N-terminal portion of a major domain of lysozyme was most unstable, similar to results of experimental studies of *solution-phase* domain fragments.[40] If folding and unfolding pathways are closely or even partly related, the similarities identified between in vacuo simulations and solution-phase experiments suggest that both kinds of studies probe mainly the intrinsic properties of the protein folds and the internal forces of the proteins, as well as that the role of the solvent is important more in changing the relative populations of different conformations or the time scale of relevant conformational changes. Only more experimentation and modeling can tell whether this hypothesis is strongly grounded.

Computer-generated extended conformers of disulfide-intact lysozyme were similar in length to disulfide-intact lysozyme in the charge state $Q = 9+$ studied by the energetic surface imprinting technique.[26] It remains to be seen whether such computer-generated species might correspond at a finer level of detail to partly unfolded gas-phase ions observed using different kinds of physical measurements.[22,26,28] For disulfide-reduced lysozyme, correspondence between the molecular dynamics centrifugal denaturation runs and studies of disulfide-reduced lysozyme ions in the gas phase was poor, perhaps because the unfolding pathways or the starting structures differed between the experiment and simulation.

Despite limitations, the GROMOS force field appears to be a reasonable starting point for representing proteins in vacuo. In the future, molecular dynamics techniques may be useful for driving proteins into unusual conformational states in vacuo by modulating parameters such as charge state and location of charged residues. Work along these lines is currently being pursued with encouraging preliminary results.

Acknowledgment. C.T.R. and O.T. are grateful for financial support from the Swedish Natural Sciences Council (NFR) and the Swedish Technical Research Council (TFR). The authors thank the anonymous referees for helpful comments and criticism.

References and Notes

(1) Karas, M.; Hillenkamp, F. *Anal. Chem.* **1988**, *60*, 2299−2301.
(2) Hillenkamp, F.; Karas, M.; Beavis, R. C.; Chait, B. T. *Anal. Chem.* **1991**, *63*, 1193A-1203A.
(3) Nelson, R. W.; Dogruel, D.; Williams, P. *Rapid Commun. Mass Spectrom.* **1994**, *8*, 627−631.
(4) Fenn, J. B.; Mann, M.; Meng, C. K.; Wong, S. F.; Whitehouse, C. M. *Science* **1989**, *246*, 64−71.
(5) Smith, R. D.; Loo, J. A.; Edmonds, C. G.; Barinaga, C. J.; Udseth, H. R. *Anal. Chem.* **1990**, *62*, 882−889.
(6) Nohmi, T.; Fenn, J. B. *J. Am. Chem. Soc.* **1992**, *114*, 3241−3246.
(7) Chen, R.; Cheng, X.; Mitchell, D. W.; Hofstadler, S. A.; Wu, Q.; Rockwood, A. L.; Sherman, M. G.; Smith, R. D. *Anal. Chem.* **1995**, *67*, 1159−1163.
(8) Jones, J. L.; Dongré, A. R.; Somogyi, A.; Wysocki, V. H. *J. Am. Chem. Soc.* **1994**, *116*, 8368−8369.
(9) Covey, T.; Douglas, D. J. *J. Am. Soc. Mass Spectrom.* **1993**, *4*, 616−623.
(10) Cox, K. A.; Julian, R. K.; Cooks, R. G.; Kaiser, R. E. *J. Am. Soc. Mass Spectrom.* **1994**, *5*, 127−136.
(11) Douglas, D. J. *J. Am. Soc. Mass Spectrom.* **1994**, *5*, 17−18.
(12) Loo, R. R. O.; Udseth, H. R.; Smith, R. D. *J. Am. Soc. Mass Spectrom.* **1992**, *3*, 695−705.
(13) Winger, B. E.; Light-Wahl, K. J.; Smith, R. D. *J. Am. Soc. Mass Spectrom.* **1992**, *3*, 624−630.
(14) Loo, R. R. O.; Smith, R. D. *J. Am. Soc. Mass Spectrom.* **1994**, *5*, 207−220.
(15) Loo, R. R. O.; Winger, B. E.; Smith, R. D. *J. Am. Soc. Mass Spectrom.* **1994**, *5*, 1064−1071.
(16) Wagner, D. S.; Anderegg, R. J. *Anal. Chem.* **1994**, *66*, 706−711.
(17) Suckau, D.; Shi, Y.; Beu, S. C.; Senko, M. W.; Quinn, J. P., Wampler, F. M., III; McLafferty, F. W. *Proc. Natl. Acad. Sci. U.S.A.* **1993**, *90*, 790−793.
(18) Wood, T. D.; Chorush, R. A.; Wampler, F. M. I.; Little, D. P.; O'Connor, P. B.; McLafferty, F. W. *Proc. Natl. Acad. Sci. U.S.A.* **1995**, *92*, 2451−2454.
(19) Tang, X.-J.; Brewer, C. F.; Saha, S.; Chernushevich, I.; Ens, W.; Standing, K. G. *Rapid Commun. Mass Spectrom.* **1994**, *8*, 750−754.
(20) Anderegg, R. J.; Wagner, D. S. *J. Am. Chem. Soc.* **1995**, *117*, 1374−1377.
(21) Cheng, X.; Morin, P. E.; Harms, A. C.; Bruce, J. E.; Ben-David, Y.; Smith, R. D. *Anal. Biochem.* **1996**, *239*, 35−40.
(22) Valentine, J. S.; Anderson, J. G.; Ellington, A. D.; Clemmer, D. E. *J. Phys. Chem. B* **1997**, *101*, 3891−3900.
(23) Mathews, C. K.; van Holde, K. E. *Biochemistry*; The Benjamin/Cummings Publishing Co., Inc.: Redwood City, Ca, 1990.
(24) Bränden, C.; Tooze, J. *Introduction to Protein Structure*; Garland Publishing, Inc.: New York, 1991.
(25) Wolynes, P. G. *Proc. Natl. Acad. Sci. U.S.A.* **1995**, *92*, 2426−2427.
(26) Reimann, C. T.; Sullivan, P. A.; Axelsson, J.; Quist, A. P.; Altmann, S.; Roepstorff, P.; Velázquez, I.; Tapia, O. *J. Am. Chem. Soc.* **1998**. Submitted for publication.
(27) Schnier, P. D.; Gross, D. S.; Williams, E. R. *J. Am. Soc. Mass Spectrom.* **1995**, *6*, 1086−1097.
(28) Gross, D. S.; Schnier, P. D.; Rodriguez-Cruz, S. E.; Fagerquist, C. K.; Williams, E. R. *Proc. Natl. Acad. Sci. U.S.A.* **1996**, *93*, 3143−3148.
(29) van Gunsteren, W. F.; Billeter, S. R.; Eising, A. A.; Hünenberguer, P. H.; Krüger, P.; Mark, A. E.; Scott, W. R. P.; Tironi, I. G. *Biomolecular Simulation: The GROMOS96 Manual and User Guide*; VDF: Zürich, 1996.
(30) Mark, A. E.; van Gunsteren, W. F. *Biochemistry* **1992**, *31*, 7745−7748.
(31) Hünenberger, P. H.; Mark, A. E.; van Gunsteren, W. F. *Proteins: Strut., Funct., Genet.* **1995**, *21*, 196−213.
(32) Åqvist, J.; van Gunsteren, W. F.; Leijonmarck, M.; Tapia, O. *J. Mol. Biol.* **1985**, *183*, 461−477.
(33) Berendsen, H. J. C.; Postma, J. P. M.; Di Nola, A.; van Gunsteren, W. F.; Haak, J. R. *J. Chem. Phys.* **1984**, *81*, 3684.
(34) Tapia, O.; Nilsson, O. In *Molecular Aspects of Biotechnology: Computational Models and Theories*; Bertrán, J., Ed.; Kluwer Academic Publishers: Netherlands, 1992.
(35) Sanejouand, Y. H.; Tapia, O. *J. Phys. Chem.* **1995**, *99*, 5698−5704.
(36) Wilson, K. P.; Malcolm, B. A.; Matthews, B. W. *J. Biol. Chem.* **1992**, *267*, 10842.
(37) Ryckaert, J.-P.; Ciccotti, G.; Berendsen, H. J. C. *J. Comput. Phys.* **1977**, *23*, 327.
(38) McCammon, J. A.; Gelin, B. R.; Karplus, M.; Wolynes, P. G. *Nature* **1976**, *262*, 325−326.
(39) Brooks, B.; Karplus, M. *Proc. Natl. Acad. Sci. U.S.A.* **1985**, *82*, 4995−4999.
(40) Yang, J. J.; van den Berg, B.; Pitkeathly, M.; Smith, L. J.; Bolin, K. A.; Keiderling, T. A.; Redfield, C.; Dobson, C. M.; Radford, S. E. *Folding Des.* **1996**, *1*, 473−484.
(41) Saenger, W. *Principles of Nucleic Acid Structure*; Springer-Verlag: New York, 1984.
(42) McCammon, J. A.; Havery, S. C. *Dynamics of Proteins and Nucleic Acids*; Cambridge University Press: Cambridge, U.K., 1987.
(43) Miranker, A.; Robinson, C. V.; Radford, S. E.; Aplin, R. T.; Dobson, C. M. *Science* **1993**, *262*, 896−900.
(44) Miranker, A.; Radford, S. E.; Karplus, M.; Dobson, C. M. *Nature* **1991**, *349*, 633−636.
(45) Chou, K.-C. *Biophys. Chem.* **1988**, *30*, 3−48.
(46) Bohr, J.; Bohr, H. G.; Brunak, S. *Europhys. News* **1996**, *27*, 50−54.